Heliyon 10 (2024) e34813

Contents lists available at ScienceDirect

Heliyon

journal homepage: www.cell.com/heliyon

Research article

Kinetic modeling of the photocatalytic degradation of acetaminophen and its main transformation products

Miguel Ángel López Zavala *, Jocelín Alí Delgado Juárez

Tecnologico de Monterrey, School of Engineering and Science, Av. Eugenio Garza Sada Sur No. 2501, Col. Tecnológico, Monterrey, N. L., C.P. 64849, Mexico

ARTICLE INFO

Keywords:
Acetaminophen
Heterogenous photocatalysis
Kinetic modeling
Monte Carlo simulation
TiO_2 nanotubes

ABSTRACT

In this study, a kinetic model of the heterogeneous photocatalytic degradation of acetaminophen and its main transformation products is presented. Kinetic photocatalytic modeling and photon absorption rate modeling were included. Monte Carlo method was used to model the photon absorption process. Experiments were carried out in a reactor operated in batch mode and TiO_2 nanotubes were used as photocatalyst irradiated with 254 nm UVC. Kinetic parameters were estimated from the experiments data by applying a non-linear regression procedure. Intrinsic expressions to the kinetics of acetaminophen degradation and its main transformation products were derived. Model, kinetics and photon absorption formulations and parameters proved to be affordable for describing the photocatalytic degradation of acetaminophen, but improvements should be done for better description of formation and oxidation kinetics of main transformation products. The model should be tested with other pharmaceuticals and emergent pollutants to calibrate it and evaluate its applicability in a wide range of compounds.

1. Introduction

Acetaminophen or paracetamol is one of the most prescribed and used drugs in the world [1,2]. Therefore, the presence of trace amounts of acetaminophen in water bodies and in drinking water is a public concern, since little is known about the possible chronic health effects associated with long-term ingestion [1]. Recently, several methods for the removal and degradation of drugs have been proposed for the remediation of aqueous systems, where advanced oxidation processes (AOPs) include a range of promising methods for the destruction of aquatic pollutants [3,4]. Among the AOPs, photocatalytic reactions employing semiconductor catalysts have demonstrated their efficiency in degrading a wide range of compounds into readily biodegradable compounds, and eventually mineralizing them to innocuous carbon dioxide and water [5]. The most common semiconductor used in photocatalysis is TiO_2, because is inexpensive, physically robust, and relatively nontoxic. Additionally, it obviates the need to continuously supply chemical precursors, which is a benefit for water treatment applications [6]. The construction of TiO_2 nanostructures with interesting morphologies and properties has recently attracted considerable attention because they present additional opportunities to improve the efficiency of the photocatalytic reaction by promoting charge migration and increasing surface area [7]. Among TiO_2 materials, nanotubes may have possessed advantages for photocatalytic reactions (in comparison with nanospheres), because they have a greater surface-volume ratio [8].

* Corresponding author. Tecnologico de Monterrey, Av. Eugenio Garza Sada Sur No. 2501, Col. Tecnológico, Monterrey, N. L., C.P. 64849, Mexico.

E-mail address: miganloza@tec.mx (M.Á. López Zavala).

https://doi.org/10.1016/j.heliyon.2024.e34813
Received 25 January 2024; Received in revised form 16 July 2024; Accepted 17 July 2024
Available online 23 July 2024

Abbreviations

AOPs	advanced oxidation processes
APAP	acetaminophen
C	concentration of acetaminophen
DO	dissolved oxygen
EC	electrical conductivity
K	adsorption constant of the catalyst
LVRPA	local volumetric rate of photon absorption
RSW	raw surface water
TOC	total organic carbon
TP	transformation product
k' (kK)	rate constant of the photocatalytic degradation
$[j_{ads}]$	concentration of the specie j adsorbed on the catalyst surface
K_j	equilibrium adsorption constant
$[site_j]$	surface concentration of vacant adsorption sites
[j]	concentration of specie j in the suspension bulk
$[site_{j,T}]$:	total concentration of sites
$[site_{j,oc}]$:	surface concentration of occupied sites by the specie j
$[j_{ads}]$	concentration of the specie j adsorbed on the catalyst surface
k_j:	kinetic constant of the reaction between the organic compound and hydroxyl radicals

Although photocatalytic processes for water treatment have been the subject of extensive research over the past three decades [6], research with reactors has been limited, slowing down the scalability and possible industrialization of this technology. The correct design of photocatalytic reactors is of paramount importance for industrial application. The scale-up of a photoreactor requires the development of mathematical models, which should be based on the reaction mechanism and should describe explicitly the effect of the radiation absorption [9,10]. Therefore, to make the practical application of the photocatalytic process for water remediation more feasible, it is necessary to develop models that predict the performance of a photocatalytic reactor.

Thus, in this work, a kinetic model is proposed to describe the degradation of acetaminophen, as well as its main transformation products (TP). The study was carried out using a photocatalytic reactor operated in a batch mode, with UVC as an energy source and TiO_2 nanotubes as a catalyst. The kinetic equations are based on mechanistic reaction steps and include the modeling of the radiation absorption. To approximate the radiation absorbed in the rector, a numerical simulation by the Monte Carlo method was used. The main target of this study is to predict acetaminophen degradation in a heterogenous photocatalytic reactor using minimal experimental data.

2. Materials and methods

2.1. Chemicals

Acetaminophen (4-acetamidophenol, 98 %) and Degussa P25 titanium dioxide (99.5 %, 88 % anatase and 12 % rutile) were obtained from Sigma-Aldrich (Toluca, Mexico). Sodium hydroxide (NaOH) and hydrochloric acid (HCl, 37 %) were purchased from Fermont (Mexico City, Mexico). Methanol was provided by J.T. Baker (Center Valley, PA).

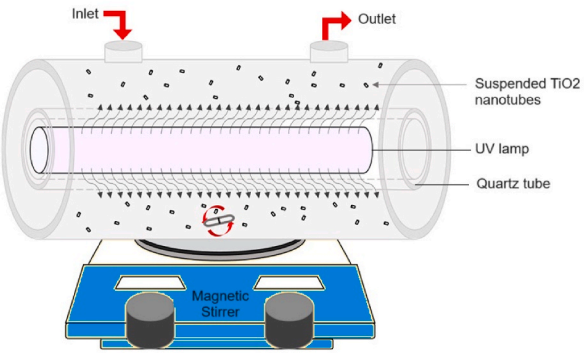

Fig. 1. Experimental device: Heterogeneous photocatalytic reactor, using TiO_2 nanotubes as a photocatalyst.

2.2. Experimental setup

Acetaminophen degradation was carried out in a 0.3 L stainless steel cylindrical photocatalytic reactor provided with a high-pressure Hg candle lamp (UV wavelength 254 nm and intensity 25 W/cm^2) manufactured by Light Sources Inc. (GPH212T5L model). The lamp is placed inside a quartz tube located in the center of the reactor which is submerged in the water solution (Fig. 1). The water solution is kept under constant agitation using a magnetic stirrer. The oxidation process is conducted at room temperature and under not pressurized conditions.

2.3. The photocatalyst: TiO_2 nanotubes

Titanium dioxide (TiO_2) nanotubes (photocatalyst) were synthesized based on the protocol reported by López Zavala et al. [11]. A suspension was prepared using 0.3 g of TiO_2 nanoparticles (Degussa P25) and 30 mL of 10 M NaOH solution. The suspension was mixed for 2 h at 30 °C and then autoclaved at 110 °C for 72 h; later, it was allowed to cool at room temperature. The suspension was centrifuged for 15 min at 4500 rpm. The supernatant was discarded, and the solids were redispersed in 200 mL of a 0.1 M HCl solution for 3 h. The suspension was centrifuged again (15 min, 4500 rpm), and the solids were recovered and subsequently washed with distilled water until the pH stabilized near neutrality. The solids were allowed to dry at 80 °C in a vacuum oven. Finally, the dried solids were annealed at 600 °C for 2 h to generate TiO_2 nanotubes with an anatase crystallographic phase.

2.4. Characterization of surface water

Raw surface water (RSW) and water samples from the experiments were characterized based on parameters such as total organic carbon (TOC), pH, electrical conductivity (EC), chlorides and acetaminophen concentration. TOC was determined based on protocol 5310 described in the standard methods for the examination of water and wastewater [12]. Electrical conductivity and pH were measured by using Thermo Scientific Orion 3-Star equipment (Thermo Fisher Scientific, Waltham, MA). Traces of acetaminophen in water samples were determined by high-performance liquid chromatography, as described in section 2.5.

2.5. Photocatalytic degradation of acetaminophen and its oxidation products

10 mg/L acetaminophen solution was prepared with raw surface water. Surface water was taken from the Rodrigo Gómez dam located near Monterrey City, Mexico. Raw surface water characteristics were pH 8.1, electrical conductivity 312 μS/cm, chlorides concentration 13.6 mg/L, and total organic carbon 3.80 mg/L. Acetaminophen traces in raw surface water were not detected at 254 nm. The initial pH of the solution was adjusted to 7 using HCl as required. The characteristics of the resulting acetaminophen solution were pH 7.01, EC 382 μS/cm, chlorides concentration 28.2 mg/L, TOC 10.64 mg/L and APAP 11.48 mg/L. Then, 300 mL of the pH 7 acetaminophen solution and 100 mg of TiO_2 nanotubes were mixed into the reactor. The mixture was stirred for 30 min under dark conditions and subsequently, the lamp was turned on and degradation started. Samples were collected at the following reaction times: 0, 1, 2.5, 5, 7.5, 10, 15, 20, 25, 30, 35, 40, 50, 60, 120 and 240 min. The collected samples were centrifuged at 4500 rpm for 15 min to separate the nanotubes and subsequently, the aqueous fractions were analyzed. All experiments were conducted on batch configuration under constant agitation, room temperature and not pressurized conditions.

TOC, pH, EC, and chlorides concentration of centrifuged aqueous fractions were determined as described in section 2.4. Traces of acetaminophen and its transformation products (TP) were determined by high-performance liquid chromatography using an Agilent 1200 HPLC-DAD system (Agilent Technologies, Santa Clara, CA). Analytes were separated by using a 150 × 4.6 mm reverse phase monomeric Zorbax C18 column with 5 μm diameter spherical particles (MAC-MOD Analytical, Wilmington, DE). The mobile phase consisted of methanol and ultrapure water in a 50:50 (v/v) proportion and the operating conditions of the equipment were temperature 30 °C, flowrate of 1.0 mL/min, detection at 254 nm and injection volume of 20 μL.

Degradation rate constants were determined regarding first-order kinetics [1,13,14]. The Langmuir-Hinshelwood model (Equation (1)) was used, where the kinetic constant is related to the decomposition and the adsorbate concentration [13]. In Equation (1), k is the rate constant, which depends on the light intensity, K is the adsorption constant of the catalyst and C is the concentration of acetaminophen. For low adsorption rates and concentrations (KC < 1), Equation (1) reduces to the first-order kinetics (Equation (2)). The separation of variables and the integration between the initial conditions t = 0 and C = C_0 at time t results in the Equation (3), where k' (kK) is the rate constant of the photocatalytic degradation. When Equation (3) is plotted, the slope corresponds to the reaction rate constant k' (units of min^{-1}).

$$\frac{dC}{dt} = -\frac{kKC}{1+KC} \tag{1}$$

$$\frac{dC}{dt} = -kKC \tag{2}$$

$$ln\left(\frac{C_0}{C}\right) = kKt = k't \tag{3}$$

The half-life of the photocatalytic degradation, which is the time to decrease the acetaminophen concentration by half is given by

Equation (4). Likewise, the efficiency of the photocatalytic degradation is determined with Equation (5), where C_f and C_0 are the initial and final acetaminophen concentrations, respectively.

$$t_{1/2} = \frac{\ln(2)}{k'} \tag{4}$$

$$\text{Efficiency of photocatalytic degradation } (\%) = \frac{(C_0 - C_f)}{C_0} \times 100 \tag{5}$$

2.6. Modeling of the heterogeneous photocatalytic reactor

The heterogeneous photocatalytic reactor was modeled following the procedure reported by Ballari et al. [15] (Fig. 2). Two stages were identified, kinetic photocatalytic modeling and photon absorption rate modeling. The last one was conducted independently of the photocatalytic kinetic modeling due to the radiation balance in the photocatalytic reactor does not depend on the concentration of the chemical species. The mass conservation equations for acetaminophen and its main transformation products were developed. To solve the mass balances, reaction rate expressions were obtained from the mechanistic kinetic scheme of a photocatalytic process. The radiation-activation step of the mechanism requires the evaluation of the electron-hole generation rate, which depends on the photon absorption rate. The photon absorption rate is a volumetric property (referred to as LVRPA), due to the reaction of the catalyst particles are in an aqueous suspension. Therefore, to evaluate the rate of photon absorption, the radiation field inside the photocatalytic reactor was computed. To do that, the boundary conditions (modeled with a lamp surface emission model) and the optical properties of the heterogeneous system were introduced. The Monte Carlo method was applied to calculate the volumetric rate of photon absorption. The LVRPA was introduced into the kinetic expressions for solving the mass balances. Some assumptions and simplifications were considered to maintain the approach as rigorous as possible, these assumptions and simplifications will be described in the following sections.

2.6.1. Photon absorption rate modeling by Monte Carlo Method

The Monte Carlo simulation prepared to describe the propagation of light in the suspension of TiO_2 nanotubes was adapted from Zekry & Colbeau-Justin [16]. The LVRPA obtained was introduced into the proposed kinetic model (section 2.6.2, "Photocatalytic kinetic model") to obtain complete simulated profiles of the degradation of acetaminophen and its TP. Fig. 3 shows the flowchart of the Monte Carlo simulation and a detailed description of photon absorption rate modeling is included as supporting information. The features of the modeled system are shown in section 2.2 "Experimental device".

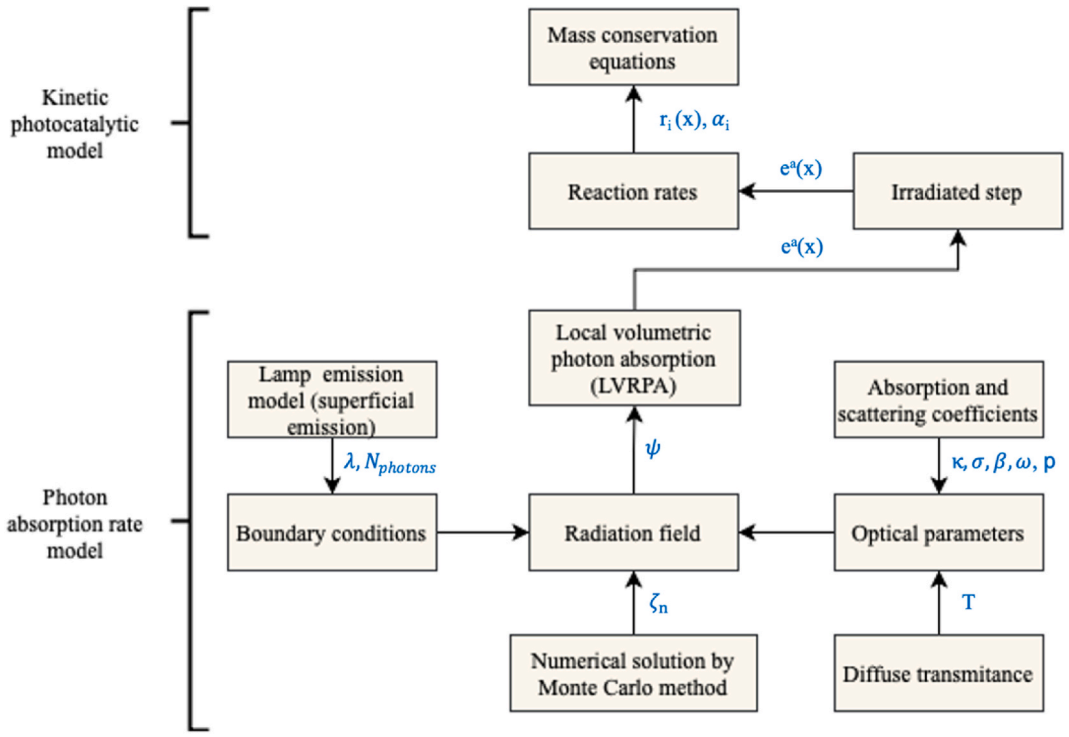

Fig. 2. Modeling and simulation of acetaminophen degradation in a heterogeneous photocatalytic reactor. Input parameters are shown in blue. Adapted from Ballari et al. [15].

Model assumptions.

i. The tubular UV lamp is modeled as a polychromatic extended source with surface emission (ESSE). This model assumes a uniform emission from the surface of the lamp and is directionally independent.
ii. The emission of the photons from the surface of the lamp is considered as a stochastic process.
iii. Photons follow a straight trajectory in the medium after being emitted from the lamp.

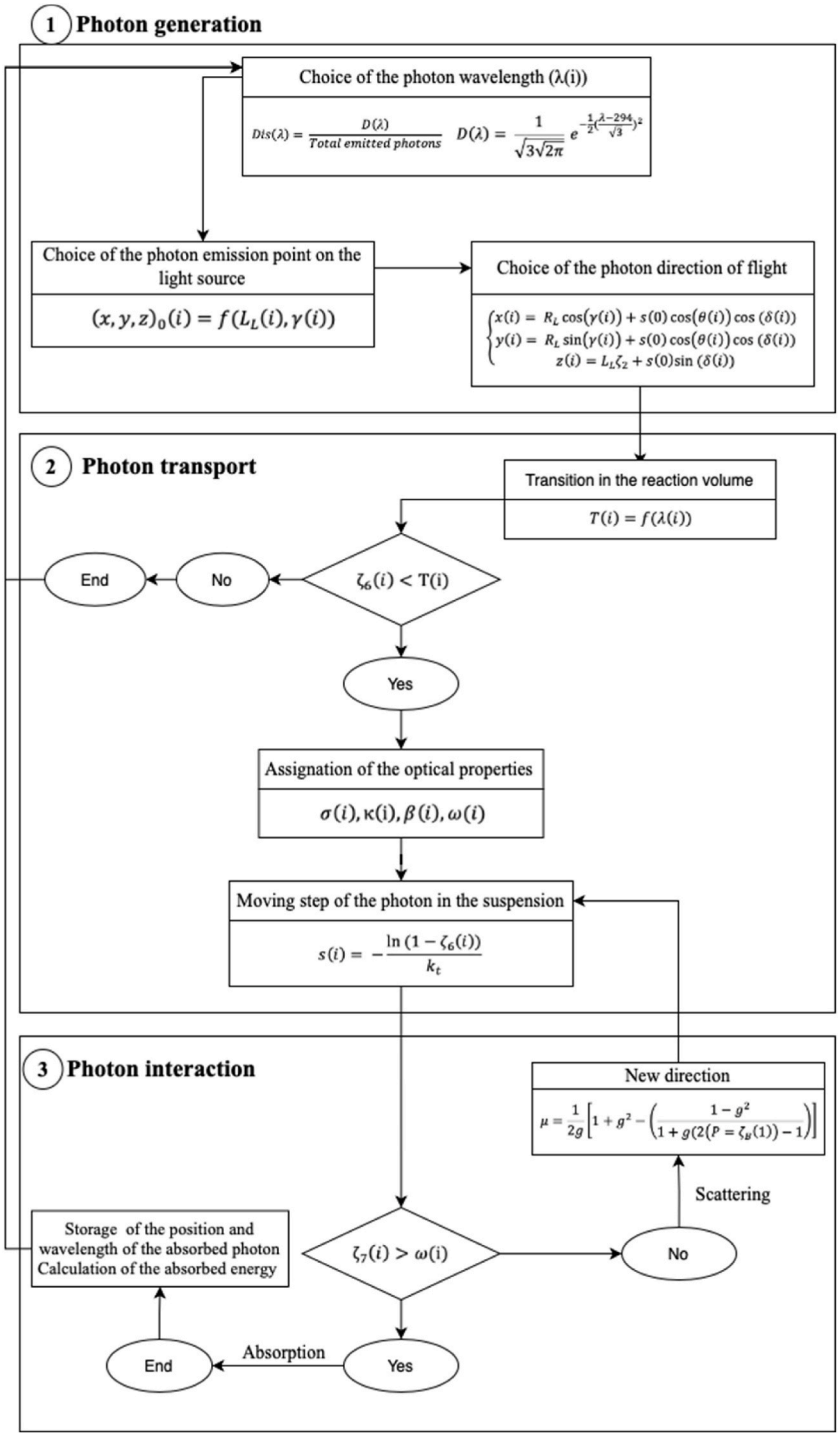

Fig. 3. Monte Carlo simulation flowchart. Adapted from Zekri & Colbeau-Justin [16].

iv. Part of the light spectrum of the lamp will fail to pass the barrier of the internal quartz tube, the probability of crossing and entering the reacting medium merges with the transmittance property.
v. For simulation, reported values of optical properties are considered.

2.6.2. Photocatalytic kinetic model

The photocatalytic kinetic model was prepared regarding only one transformation product (TP) based on the results of a previous study reported by Lozano-Morales et al. [13] for acetaminophen photocatalytic degradation with TiO_2 nanotubes. The mass balance for the photocatalytic system that dictates the behavior of the concentration of acetaminophen and its TP is introduced in the following section "Mass balance". To solve the mass balance and to know the degradation rates of the organic compounds, a mechanistic model was developed and presented in the section entitled "Mechanistic derived photocatalytic kinetic model". The kinetic model was prepared based on the models reported by Manassero et al. [17] and Satuf et al. [18]. In the mechanistic kinetic model, the absorption of photons is included in the radiation-activation step, this value (LVRPA) was determined by applying the Monte Carlo method described in section 2.6.1 "Photon absorption rate modeling by Monte Carlo Method".

2.6.2.1. Mass balance. The modeled system was a cylindrical reactor operated in a batch type mode. The general mass balance around the system is represented by Equation (6), where $[C_j]$ is the molar concentration of the constituent j, t is t the reaction time, a_v is the catalytic surface area per unit of suspension volume (computed from the product of the catalyst specific surface area and the catalyst loading), and $r_X(x,t)$ is the reaction rate. The mass balance of the system assumes that conversion of analytes over time is differential, the solution is well mixed and there are no limitations on mass transport, photocatalytic reactions only occur on the surface of the catalyst and there is no photolysis in the process.

$$\frac{d[C_j]}{dt} = -a_v\{\langle r(x,t)\rangle\} \tag{6}$$

To obtain the theoretical evolution of the acetaminophen (APAP) concentration and its main TP, it is necessary to solve the mass balance for each specie. The mass balances for the species are solved in Equations (7)–(9) and are based on the acetaminophen degradation pathway shown in Fig. 4. In Fig. 4 it is proposed that APAP is degraded and forms a major transformation product, which is subsequently mineralized. In Equations (7)–(9), r_{APAP} represents the reaction rate of APAP and r_{TP1} represents the reaction rate of the transformation product.

$$\frac{d[APAP]}{dt} = -a_v\{\langle r_{APAP}(x,t)\rangle\} \tag{7}$$

$$[APAP](t=0) = [APAP]$$

$$\frac{d[TP1]}{dt} = a_v\{\langle r_{APAP}(x,t)\rangle - \langle r_{TP1}(x,t)\rangle\} \tag{8}$$

$$[TP1](t=0) = 0$$

$$\frac{d[CO_2]}{dt} = a_v\{\langle r_{TP1}(x,t)\rangle\} \tag{9}$$

$$[CO_2](t=0) = 0$$

The mass balances (Equations (7)–(9)) are presented as a set of differential equations dependent on two variables: concentration of the compounds (x) and reaction time (t). The specific concentration of the compounds at a specific time is determined by the dependance on the concentration of the other compounds. Thus, the rate of generation of TP_1 and CO_2 depends on the rate of consumption of APAP, so the rate of TP_1 and CO_2 also depends on the initial input of x and t. The solution of the differential equation system was approximated from a recursive computational solution. The approximation of the values to subsequently execute the recursive steps, depends on the initial concentrations, which are theoretically: $x_{APAP} = 10$ mg/L and x_{TP_1} and $x_{CO_2} = 0$ mg/L. Also, it is

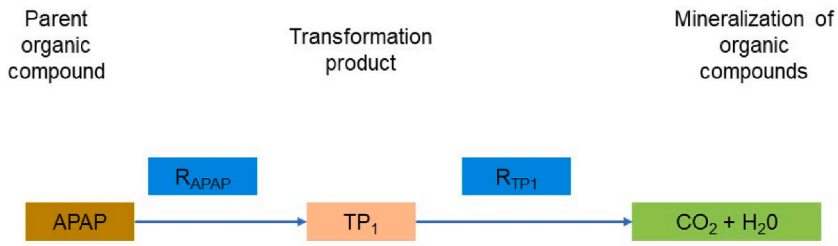

Fig. 4. Reaction pathway for the APAP degradation.

necessary to make assumptions about the general behavior of the reaction so that the established differential equations faithfully represent the reaction. As shown in Fig. 4, the model assumes that APAP degrades only and directly into an intermediate product, which is fully mineralized. Therefore, the experimental degradation rate is an input for the calculation of the other rates. Likewise, as it is a recursive method that solves a system of equations, the rate, being an input, will be adjusted as feedback is received from the execution of the solution.

2.6.2.2. Mechanistic derived photocatalytic kinetic model. The kinetic model involved the establishment of a general photocatalytic mechanism for the degradation of APAP and TP_1. The mechanism proposed in this work involved an activation step, an adsorption balance of the organic compounds and the photocatalytic reaction, carried out on the surface of the catalyst. Although the oxidation of organic compounds can occur mainly by three pathways, superoxide ions ($O_2^{\bullet -}$), hydroxyl radicals ($^{\bullet}OH$) and other reactive oxygen species (ROS), which can compete with each other; normally, one of the pathways is proposed as the dominant, which is regularly agreed to be the degradation by hydroxyl radicals [19]. Table 1 shows the reactions (elemental steps) of the photocatalytic mechanism followed to evaluate the degradation of APAP and the formation and degradation of TP_1. For simplifying the mechanism, only the degradation of APAP and TP_1 by hydroxyl radicals is considered.

To obtain the rate expressions, the following assumptions were made [17].

a) Photocatalytic reactions occur on the catalyst surface and occur with the adsorbed species.
b) Before the photocatalytic reaction, there is already a dynamic equilibrium between the mass and adsorbed concentrations of H_2O, O_2 and organic and inorganic compounds.
c) It is postulated that exists a competitive adsorption mechanism between APAP and TP_1.
d) Molecular oxygen (O_2) and organic compounds (APAP and TP_1) are adsorbed on different sites of the catalyst surface.
e) Hydroxyl radical attack is the dominant degradation pathway for APAP and TP_1
f) The concentration of water molecules and hydroxyl ions on the catalyst surface remains constant.
g) There are no limitations to the mass transport [20].
h) O_2 concentration is constant and in excess concerning the stoichiometric demand. Although dissolved oxygen (DO) was not injected into the photocatalytic reaction, the reaction was not under anoxic conditions because constant stirring conditions were kept. Therefore, this assumption was made to prevent all the recombination of "e^{-}", since O_2 acts as an electron scavenger, allowing the valence band hole to generate hydroxyl radicals [5], giving rise to the assumed main pathway degradation (assumption e)).
i) The concentration of total absorption sites of APAP, per unit area of catalyst, can be considered constant.
j) The surface rate of electron-hole generation (r_{gs}) is given by the Equation (10), where Φ is the quantum efficiency, determined with the Equation (11) [21] and $\int_{\lambda} e_{\lambda}^{a}(x)d\lambda$ is the LVRPA.

$$r_{gs} = \frac{\Phi}{a_v}\int_{\lambda} e_{\lambda}^{a}(x)d\lambda \tag{10}$$

$$\Phi = \frac{[\text{reaction rate of species j}]}{[\text{rate of photon absorption by the species to be activated}]} \tag{11}$$

Assumptions a) to d) refer to the adsorption equilibrium of the compounds on the catalyst surface. The adsorbed surface concentration of the species can be expressed with the Langmuir competitive adsorption model, which is linear for low concentrations [19]. The adsorbed surface concentration of APAP, TP_1 and O_2 was expressed as shown in Equations (12)–(14), respectively. In the equations $[j_{ads}]$ represents the concentration of the specie j adsorbed on the catalyst surface, K_j is the equilibrium adsorption constant, $[site_j]$ represents the surface concentration of vacant adsorption sites, and $[j]$ is the concentration of specie j in the suspension bulk.

$$[APAP_{ads}] = K_{APAP}[site_{APAP}][APAP] \tag{12}$$

Table 1
Reactions involved in the heterogeneous photocatalytic degradation of APAP and TP_1 by hydroxyl radicals ($^{\bullet}OH$).

Stage	Reaction	Rates and constants
Activation	$TiO_2 + h\nu \rightarrow e^- + h^+$	r_{gs}
Recombination	$e^- + h^+ \rightarrow e^- + heat$	$k_2[e^-][h^+]$
Electron trapping	$e^- + O_{2,\,ads} \rightarrow O_2^{\bullet -}$	$k_3[e^-][O_{2,\,ads}]$
Hole trapping	$h^+ + H_2O_{ads} \rightarrow {}^{\bullet}OH + H^+$	$k_4[h^+][H_2O_{ads}]$
	$h^+ + OH^-_{ads} \rightarrow {}^{\bullet}OH$	
Hydroxyl attack	$APAP_{ads} + {}^{\bullet}OH \rightarrow TP_1$	$r_{APAP=}k_5[APAP_{ads}][{}^{\bullet}OH]$
	$TP_{1,ads} + {}^{\bullet}OH \rightarrow CO_2 + H_2O$	$r_{TP1=}k_6[TP_{1,ads}][{}^{\bullet}OH]$
Adsorption	$site_{O2} + O_2 \leftrightarrow O_{2,\,ads}$	K_{O2}[a]
	$site_{H2O} + H_2O \leftrightarrow H_2O_{ads}$	K_{H2O}[a]
	$site_{H2O} + H_2O \leftrightarrow OH^-_{ads} + H^+$	
	$site_{APAP} + APAP \leftrightarrow APAP_{ads}$	K_{APAP}[a]
	$site_{TP} + TP_1 \leftrightarrow TP_{1,ads}$	K_{TP1}[a]

[a] Constants.

$$[TP_{1,ads}] = K_{TP}[site_{APAP}][TP_1] \tag{13}$$

$$[O_{2,ads}] = K_{02}[site_{O2}][O_2] \tag{14}$$

It was assumed that the adsorption of the species is in equilibrium and a balance of sites was made (Equations (15)–(18)). Performing the balance of sites, we can relate the concentration of the vacant sites to the total concentration of sites $[site_{j,T}]$. As it was considered that the O_2 was absorbed in different sites from the organic compounds (assumption (d)), the O_2 sites available are shown in Equation (17) and the organic compounds (APAP/TP_1) sites available in Equation (18). Equations (15) and (16), $[site_{j,oc}]$ represents the surface concentration of occupied sites by the specie j.

$$[site_{O2,T}] = [site_{O2,oc}] + [site_{O2}] \tag{15}$$

$$[site_{APAP,T}] = [site_{APAP,oc}] + [site_{APAP}] \tag{16}$$

$$[site_{APAP,T}] = [APAP_{ads}] + [TP_{1,ads}] + [site_{APAP}]$$

$$[site_{O2}] = \frac{[site_{O2,T}]}{K_{O2}\,[O_2] + 1} \tag{17}$$

$$[site_{APAP}] = \frac{[site_{APAP,T}]}{K_{APAP}\,[APAP] + K_{TP}\,[TP_1] + 1} \tag{18}$$

Regarding assumption e), the surface degradation rate of APAP and TP_1 through the hydroxyl radical attack pathway can be expressed with the general formula shown in Equation (19), where r_j is the reaction rate of the specie j, k_j is the kinetic constant of the reaction between the organic compound and hydroxyl radicals, [•OH] is the concentration of hydroxyl radicals on the surface of the TiO_2 nanotubes, and $[j_{ads}]$ represents the concentration of the specie j adsorbed on the catalyst surface. Therefore, based on the degradation pathway shown in Fig. 4 and the reactions described in Table 1, the degradation rate expressions of APAP and TP_1 are expressed by Equations (19)–(21).

$$r_j = k_j[^{\cdot}\mathrm{O\ H}][j_{ads}] \tag{19}$$

$$r_{APAP} = k_5[APAP_{ads}][^{\cdot}OH] \tag{20}$$

$$r_{TP1} = k_6[TP_{1,ads}][^{\cdot}OH] \tag{21}$$

To evaluate the degradation rate of the organic compounds (APAP and TP_1), the hydroxyl radical concentration $[^{\cdot}OH]$ should be expressed in terms of measurable variables. Therefore, the Micro Steady State (MSS) approximation was applied to express the surface rate of the appearance and disappearance of electrons, holes, and hydroxyl radicals (shown in Table 1), obtaining the Equations (22)–(25), respectively. Operating with these equations, the concentration of hydroxyl radicals was obtained as shown in Equation (25).

$$r_{e^-} = r_{gs} - k_2[e^-][h^+] - k_3[e^-][O_{2,ads}] \approx 0 \tag{22}$$

$$r_{h^+} = r_{gs} - k_2[e^-][h^+] - k_4[h^+][H_2O_{ads}] \approx 0 \tag{23}$$

$$r_{OH} = k_4[h^+][H_2O_{ads}] - k_5[APAP_{ads}][^{\cdot}OH] - k_6[TP_{1,ads}][^{\cdot}OH] \approx 0 \tag{24}$$

$$[^{\cdot}OH] = \frac{k_3k_4\,[H_2O_{ads}][O_{2,ads}]\left\{-1 + \sqrt{\frac{1+4k_2\,r_{gs}}{k_3k_4\,[H_2O_{ads}][O_{2,ads}]}}\right\}}{2k_2\{k_5[APAP_{ads}] + k_6[TP_{1,ads}]\}} \tag{25}$$

Considering assumptions (f) – (i) and using the previous equations, the degradation rates of APAP and TP_1 were determined. The degradation rate of APAP was calculated by substituting the Equations (12) and (25) in the Equation (20), obtaining Equation (26). The degradation rate of TP_1 was determined by substituting the Equations (13) and (25) in the Equation (21), obtaining Equation (27). α_n represents the kinetic expression that describes the rate of degradation of the organic compounds. The corresponding α_n are shown in Equations (28)–(32).

$$r_{APAP} = \frac{\alpha_1[APAP](x,t)\left(1 - \sqrt{1 + \frac{\alpha_2}{a_v}\int_\lambda e^a_\lambda(x,t)}\right)}{1 + \alpha_3[APAP](x,t) + \alpha_4[TP_1](x,t)} \tag{26}$$

$$r_{TP1} = \frac{\alpha_5[TP_1](x,t)\left(1-\sqrt{1+\frac{\alpha_2}{a_v}\int_\lambda e^a_\lambda(x,t)}\right)}{1+\alpha_3[APAP](x,t)+\alpha_4[TP_1](x,t)} \tag{27}$$

$$\alpha_1 = \frac{k_3k_4k_5[H_2O_{ads}]\left[O_{2,ads}\right]\left[site_{APAP,T}\right]K_{APAP}}{2k_2} \tag{28}$$

$$\alpha_2 = \frac{4k_2\Phi}{k_3k_4[H_2O_{ads}]\left[O_{2,ads}\right]} \tag{29}$$

$$\alpha_3 = k_5K_{APAP}\left[site_{APAP,T}\right] \tag{30}$$

$$\alpha_4 = k_6K_{TP1}\left[site_{APAP,T}\right] \tag{31}$$

$$\alpha_5 = \frac{k_3k_4k_6[H_2O_{ads}]\left[O_{2,ads}\right]\left[site_{APAP,T}\right]K_{TP1}}{2k_2} \tag{32}$$

2.6.2.3. Kinetic parameters estimation. The kinetic parameters were approximated from a least squares optimization, as suggested by Manassero et al. [17]. The values of the kinetic parameters generated by the optimization procedure were those that minimize the differences between the experimental concentrations of APAP and TP_1 and those predicted by the model. As a result of the optimization and due to the low concentration, the surface reaction rate of APAP and TP_1 follows a first-order kinetics (as deduced by Ref. [19]); therefore, $\alpha_3[APAP](x,t)+\alpha_4[TP_1](x,t) \ll 1$. Thus, the reaction rates can be rewritten as shown in Equations (33) and (34).

$$r_{APAP} = \alpha_1[APAP](x,t)\left(-1+\sqrt{1+\frac{\alpha_2}{a_v}\int_\lambda e^a_\lambda(x,t)}\right) \tag{33}$$

$$r_{TP1} = \alpha_3[TP](x,t)\left(-1+\sqrt{1+\frac{\alpha_2}{a_v}\int_\lambda e^a_\lambda(x,t)}\right) \tag{34}$$

3. Results and discussion

3.1. Photocatalytic degradation of acetaminophen

Fig. 5 shows the acetaminophen decay when photocatalytic degradation was conducted. As seen, the compound was almost totally oxidized in 240 min reaction time (99.2 %), but at 120 min 96.1 % of the acetaminophen had been already degraded. With these data, the reaction rate constant (k') and the half-life of the photocatalytic degradation of acetaminophen were estimated using Equations (3) and (4), resulting values of $k' = 0.021\ min^{-1}$ and $t_{1/2} = 33.16$ min. The reaction rate constant in this study is a little bit lower than that reported in a previous study by Lozano-Morales et al. [13], who also evaluated the photocatalytic degradation of APAP with TiO_2 nanotubes (lamp emission at $\lambda = 254$ nm, nanotubes load 0.4 g/L) in solutions at different pH conditions, obtaining a reaction rate constant $k' = 0.03\ min^{-1}$ for pH 7. The difference in the reaction rate constant should be associated with the lower amount of TiO_2 nanotubes used in this study (0.33 g/L), i.e. lower photocatalytic activity. However, the reaction rate constant obtained in this work is greater than that reported by Yang et al. [14] ($k' = 0.01\ min^{-1}$) for acetaminophen degradation using TiO_2 nanospheres (Degussa P25) at $\lambda = 254$ nm; this difference was linked to the greater photocatalytic activity of nanotubes in comparison with that of nanospheres due to the greater surface area of nanotubes. Studies have reported the effect of TiO_2 particles (not nanotubes) loading on the degradation efficiency of APAP [2,14]; Yang et al. found that efficiency begins to decrease up to TiO_2 loading of 5 g/L (4 μM of APAP concentration) [14]. However, these kinds of studies are mostly independent, and a direct comparison cannot be made, as the working

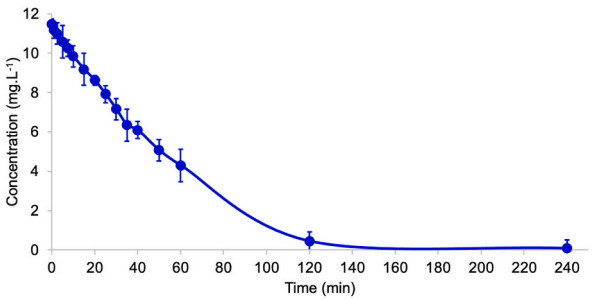

Fig. 5. Photocatalytic degradation of APAP. Initial concentration: 11.48 mg/L. The figure shows the average of three replicates.

reactor, radiation fluxes, intensity and wavelengths used are different. Therefore, the optimal catalyst loading for efficient photo-mineralization varies and depends mainly on the size of the photoreactor, as well as the properties of the catalyst used. At high concentrations of TiO_2, the nanotubes aggregate causing a light screening effect and decrease of the surface area [5]. The scattering light has a practical limit when using high concentrations of TiO_2 particles, above which the degradation rate will decrease due to the reduction of the photonic flux within the irradiated solution [22].

3.2. Photocatalytic degradation of acetaminophen transformation products

Chromatograms of Fig. 6 show the acetaminophen degradation, the formation of the transformation products and their degradation. This figure shows only the chromatograms obtained at 0, 120, and 240 min reaction time. As seen, the chromatogram at the reaction time t = 0 min (Fig. 6a) shows the peak of the APAP at 1.6 min detention time and small peaks associated to other surface water constituents. Photocatalytic degradation of acetaminophen generated mainly one transformation product (TP_1, 1.2 min) and traces of other products that had to be also degraded due to their potential toxicity. TP_1 appeared 5 min after the acetaminophen degradation started and its concentration increased gradually up to reach the maximum detection at 120 min reaction time (Fig. 6b), where the APAP was almost totally degraded (96.1 %); then, its detection decreased gradually until the end of the experiment; TP_1 was not completely degraded after 240 min of the reaction, but its detection level was quite low (Fig. 6c). Traces of other transformation products can be observed in the chromatograms; however, the area of the peaks is negligible. Lozano-Morales et al. [13] also obtained a single transformation product when APAP was photocatalytically degraded using TiO_2 nanotubes. Yang et al. [23] detected the formation of three transformation products when APAP was oxidized with TiO_2 nanospheres (Degussa P25). They reported that the main degradation pathway was through hydroxyl radicals and the three transformation compounds detected were, N-(3,4-dihydroxyphenyl) acetamide, N-(2,4-dihydroxyphenyl) acetamide, and hydroquinone. Early presence of these three compounds is expected as they comprise the basic structure of APAP. Therefore, the transformation products detected in this study could be those reported by Yang et al. [23]. Fig. 7 summarizes the evolution of photocatalytic degradation of APAP and the generation of the transformation product TP_1.

3.3. Total organic carbon (TOC) reduction

Confirmation of acetaminophen degradation was done by measuring reduction of total organic carbon. In the experiment, the initial TOC concentration remained constant during the first 10 min and then showed a slight decrease during the first 120 min (13.39 % reduction). The TOC reduction obtained after 240 min reaction time was 46.6 %. This result indicates that organic constituents of the APAP solution were oxidized, but the CO_2 gas generated in the reaction probably remained dissolved or transformed into carbonic acid in the solution and counted during the TOC analysis. The TOC removal rate constant obtained in this work was on the order of 2.2×10^{-3} min^{-1}. Yang et al. [14] obtained a TOC reduction of 60 % after 300 min reaction time, which follows the result obtained in this work.

3.4. Approximation of LVRPA by the Monte Carlo method

The Monte Carlo method has been effective in different works to simulate the radiation field in a photocatalytic reactor and obtain an approximation of the LVRPA [16,24,25,26,27]. In the simulation carried out in this work, a photon absorption rate (ψ) of 0.997 and a mean LVRPA of 1.76×10^{-8} E cm^{-3} s^{-1} were obtained. The numerical solution of the LVRPA could not be compared or adjusted with experimental observations of the radiation field of the system, so the shown value is assumed as an approximation to the real value.

For estimating the radiation field in the Monte Carlo simulation, boundary conditions that simulate the input of the light source and optical properties (Table 1, supporting information) of the TiO_2 nanospheres (Degussa P25) were introduced. The boundary conditions introduced correspond to a polychromatic extended source with surface emission. The surface emission was modeled with a specular emission, in which the magnitude of the light intensity vectors is independent of the angle of emission. Specular emission has been reported as typical behavior of mercury arc lamps [27]. On the other hand, the optical properties used in the study were those of Degussa P25 and not of TiO_2 nanotubes because of the lack of information in the literature for this type of structure. Despite Degussa

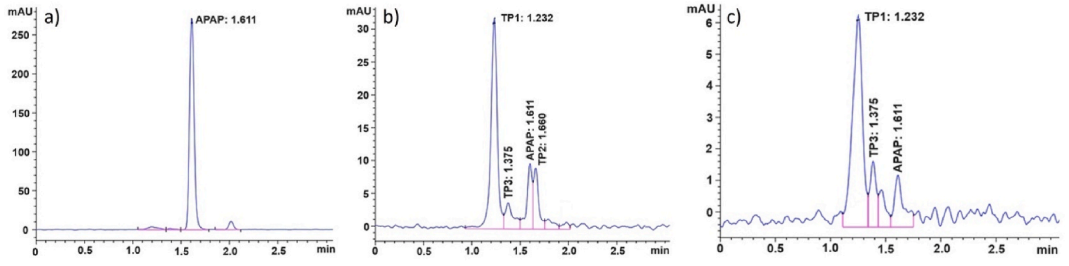

Fig. 6. Chromatograms of photocatalytic degradation of acetaminophen and its transformation products at different reaction times. (a) tr = 0 min; (b) tr = 120 min; (c) tr = 240 min. TP refers to transformation products.

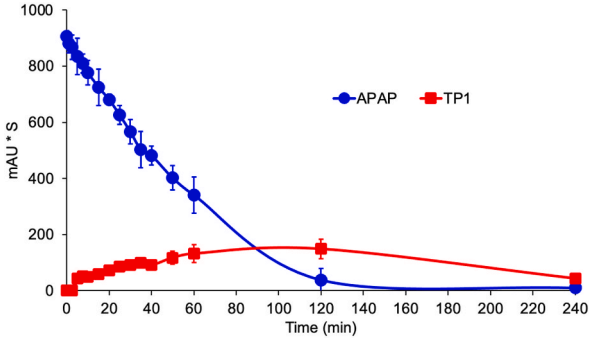

Fig. 7. Photocatalytic degradation of APAP and the transformation product TP_1. The figure depicts the average of three replicates.

P25 nanospheres were the precursor to synthesize the nanotubes and both have the same chemical structure, different morphology and particle size change the optical properties, affecting the overall photocatalytic behavior and consequently the absorbed radiation [28]. Likewise, in aqueous systems, the concentration of the catalyst, its agglomeration and the pH change the optical properties [29]. However, even though there are several conditions under which TiO_2 has different optical properties, they present similar responses over the wavelength range investigated [24,30,31].

To evaluate the absorption of photons throughout the reactor, the absorption rate of the photons in their transition from the lamp to the reactor walls was simulated. Fig. 8 shows the percentage of photon absorption rate as a function of the distance equivalent to the emission radius (radial profile). This figure shows that the absorption takes place mainly in the part closest to the lamp, exhibiting a uniform drop as the radial profile increases. For the distance of 0.4 cm after a photon leaves the lamp, its theoretical absorption disappears completely. However, this is under conditions of uniform and efficient agitation of the suspension in the reactor.

It should be mentioned that the photon absorption rate is dependent on the concentration of the photocatalyst, so when the concentration is higher, the particles closest to the radiation source absorb most of the radiation, developing a highly irradiated area near the lamp with dark areas near the walls. This would create a decrease in the real irradiated volume, considered a dead volume where no photocatalytic degradation takes place. The increase in dead volume, which is proportional to the photocatalytic load, would explain the near stagnation or decrease in photoactivity despite better overall light absorption. Therefore, the efficiency of a photocatalytic system not only depends on the amount of energy absorbed but also on its distribution in the irradiated volume [16].

The Monte Carlo simulation allows evaluating different concentrations of the photocatalyst to approximate an optimal concentration, determined by the efficient absorption of photons to carry out the photocatalytic reaction. Fig. 9 shows the relationship of the average LVRPA with catalyst loading. Initially, LVRPA increased with the catalyst loading, however, after 0.24 g/L, the LVRPA became constant irrespective of the catalyst loading. From the radiation absorption point of view, this value (0.24 g/L) can be considered the optimal catalyst concentration, so higher values than this should not be relevant for photon absorption. However, the optimal concentration value can be very different. This is because the optimum catalyst loading is not determined solely by the optical properties of the reacting medium, but also depends on the operating parameters under which the reaction is being carried out, such as the pH, which may cause agglomeration and possibly change the optical characteristics of the medium itself [27]. Therefore, it is not possible to predict an optimum catalyst loading from radiation absorption rate calculations. Nonetheless, this approach can be useful to approximate the parameters to be evaluated in a specific photocatalytic process.

Although Figs. 8 and 9 cannot determine the optimal photocatalyst concentration for efficient photon absorption, they can give an idea of what might be happening in the reactor. The increase in the photocatalyst concentration and a non-uniform agitation could have caused agglomeration of the catalyst and generation of dead volume in which the TiO_2 nanotubes were not activated. Likewise, as shown in Fig. 9, at 0.33 g/L (TiO_2 nanotubes loading used in this study), the absorption of photons is already constant, therefore, theoretically a lower concentration of catalyst could be used and still have the same LVRPA results. However, to obtain the optimal concentration for this specific reactor, an experimental evaluation of the TiO_2 nanotubes loading is necessary.

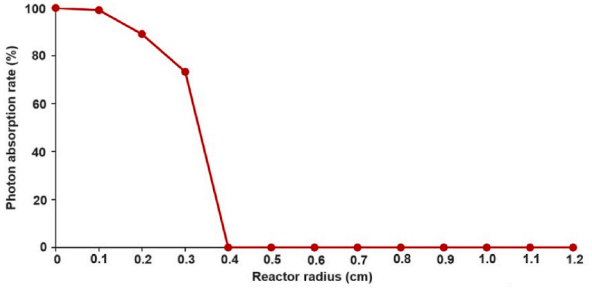

Fig. 8. Photon absorption rate as a function of the reactor radius.

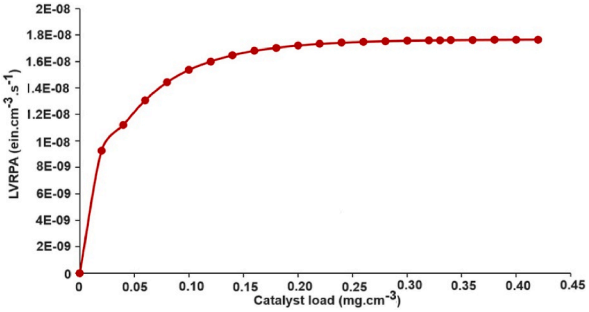

Fig. 9. LVRPA as a function of the catalyst load.

3.5. Photocatalytic kinetic model

The kinetic model was developed regarding the photocatalytic degradation of APAP was done just by hydroxyl radicals; however, it was adjusted with the experimental kinetic constant of APAP degradation (k_5 = experimental degradation constant of APAP). Kinetic parameters were determined by the least squares optimization method involving the Equations (26)–(32). The optimization renders the parameter values that minimize the values between the predicted concentrations and the experimental data. The optimization results showed that under the operating conditions of the reactor (low concentrations), the terms α_3 and α_4 of the kinetic equations could be eliminated. Therefore, the final kinetic expressions employed for the parameter's estimation were those shown in the Equations (33) and (34). Table 2 shows the estimated values of the intrinsic kinetic parameters that integrates some of the kinetic constants that can be assumed to remain constant.

The intrinsic kinetic parameters can be used for estimating the photocatalytic degradation of APAP for different concentrations and times. Fig. 10 shows the experimental concentration of APAP and the estimated concentrations of APAP and TP_1 predicted by the model under the same conditions of the reaction carried out experimentally. The green and red curves in Fig. 10 show the behavior of the solution of the differential equations that describe the reactor. Acetaminophen degrades to a transformation product (TP_1), which then mineralizes, resulting in an increase in the amount of CO_2 in the reactor. The blue line represents the experimental results of APAP degradation. As seen, the degradation rate of acetaminophen in the first 90 min of the experiment is slightly greater than the simulated results; however, in general, the behavior predicted by the model fits properly to the experimental results. Therefore, the kinetic model introduced in this study is affordable for describing the photocatalytic degradation of acetaminophen and its transformation products. Experimental results of TP_1 are not included in this figure because this transformation product was not identified and quantified, just detected as seen in Fig. 7. As observed, the pattern showed by TP_1 in Fig. 7 is smother than that presented in Fig. 10, especially at the beginning of the experiment; therefore, further work is necessary to identify and quantify the TP_1 and then estimate its experimental kinetic rate constant (k_6) to recalculate the kinetic parameters by least squares optimization method involving the Equations (26)–(32). Identification and quantification of TP_1 was out of the scope of this work.

4. Conclusions

A photocatalytic kinetic model for describing the degradation of APAP and its main transformation product was carried out. In the proposed model, only the oxidation of organic compounds by hydroxyl radicals was considered. The model was mechanistically developed with elementary steps of the photocatalytic process. The simulation of the radiation field in the reactor was carried out by the Monte Carlo method and the LVRPA was estimated. The intrinsic kinetic expressions that describe the photocatalytic reaction were obtained. Results predicted by the photocatalytic kinetic model fitted properly to those obtained experimentally for APAP degradation; but for the TP_1 kinetics more work is needed to have a more precise description of transformation products generation and oxidation. However, the effort done until now on mathematics formulations and simulation will facilitate future work to describe not only photocatalytic kinetics, oxidation mechanisms and photon absorption but also to evaluate the effect of different parameters and variables related to the photocatalyst loading, type and concentration of emergent contaminants and water characteristics. Furthermore, the use of the model for designing and scaling up the photocatalytic process is one of the most relevant future applications.

CRediT authorship contribution statement

Miguel Ángel López Zavala: Writing – review & editing, Writing – original draft, Visualization, Validation, Supervision, Resources, Project administration, Methodology, Funding acquisition, Formal analysis, Data curation, Conceptualization. **Jocelín Alí Delgado Juárez:** Validation, Software, Investigation, Formal analysis.

Declaration of competing interest

The authors declare that they have no known competing financial interests or personal relationships that could have appeared to

Table 2
Kinetic constants solved by least squares method.

Parameter	Value	Kinetic constants involved
α_1 (cm s^{-1})	5.8×10^{11}	$k_2k_3k_4k_5K_{APAP}$
α_2 (s cm^2 $eins^{-1}$)	1.67×10^{14}	$k_2k_3k_4$
α_5 (cm s^{-1})	5.24×10^{-4}	$k_2k_3k_4k_6K_{TP}$

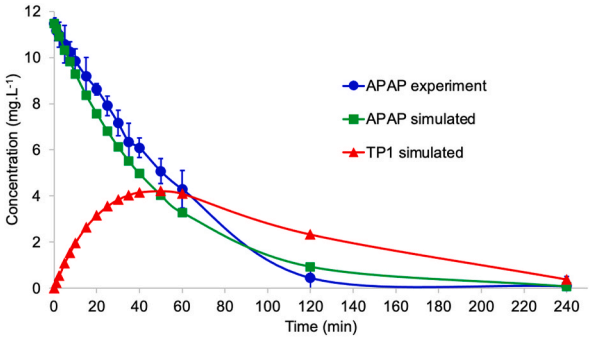

Fig. 10. Acetaminophen photocatalytic degradation. Blue line and markers show the experimental results. Green and red lines and markers correspond to the predicted degradation of APAP and TP_1, respectively, over the time course of the reaction. The initial concentration of APAP = 11.48 mg/L.

influence the work reported in this paper.

Acknowledgments

We acknowledge the support received from the National Council of Humanities, Science and Technology (CONAHCYT) of Mexico and the Tecnologico de Monterrey.

Appendix A. Supplementary data

Supplementary data to this article can be found online at https://doi.org/10.1016/j.heliyon.2024.e34813.

References

[1] N. Jallouli, K. Elghniji, H. Trabelsi, M. Ksibi, Photocatalytic degradation of paracetamol on TiO2 nanoparticles and TiO2/cellulosic fiber under UV and sunlight irradiation, Arab. J. Chem. 10 (2) (2017) S3640–S3645.
[2] X. Zhang, F. Wu, X.W. Wu, P. Chen, N. Deng, Photodegradation of acetaminophen in TiO2 suspended solution, J. Hazard Mater. 157 (2–3) (2008) 300–307.
[3] S. Esplugas, J. Giménez, S. Contreras, E. Pascual, M. Rodríguez, Comparison of different advanced oxidation processes for phenol degradation, Water Res. 36 (4) (2002) 1034–1042.
[4] R. Andreozzi, V. Caprio, A. Insola, R. Marotta, Advanced oxidation processes (AOP) for water purification and recovery, Catal. Today 53 (1) (1999) 51–59.
[5] M.N. Chong, B. Jin, C.W.K. Chow, C. Saint, Recent developments in photocatalytic water treatment technology: a review, Water Res. 44 (10) (2010) 2997–3027.
[6] S.K. Loeb, et al., The technology horizon for photocatalytic water treatment: sunrise or sunset? Environ. Sci. Technol. 53 (6) (2019) 2937–2947.
[7] M. Ge, et al., One-dimensional TiO 2 nanotube photocatalysts for solar water splitting, Adv. Sci. 4 (1) (2017) 1–31.
[8] M. Patel, R. Kumar, K. Kishor, T. Mlsna, C.U. Pittman, D. Mohan, Pharmaceuticals of emerging concern in aquatic systems: chemistry, occurrence, effects, and removal methods, Chem. Rev. 119 (6) (2019) 3510–3673.
[9] J. Schneider, et al., Understanding TiO2photocatalysis: mechanisms and materials, Chem. Rev. 114 (19) (2014) 9919–9986.
[10] O. Sacco, V. Vaiano, D. Sannino, Main parameters influencing the design of photocatalytic reactors for wastewater treatment: a mini review, J. Chem. Technol. Biotechnol. 95 (10) (2020) 2608–2618.
[11] M.Á. López Zavala, S.A. Lozano-Morales, M. Ávila-Santos, Synthesis of stable TiO2 nanotubes: effect of hydrothermal treatment, acid washing and annealing temperature, Heliyon 3 (11) (2017) e00456.
[12] APHA, Standard Methods for the Examination of Water and Wastewater, twenty-first ed., American Public Health Association/American Water Works Association/Water Environment Federation, Washington DC, 2005.
[13] S.A. Lozano-Morales, G. Morales, M.Á. López Zavala, A. Arce-Sarria, F. Machuca-Martínez, Photocatalytic treatment of paracetamol using TiO2 nanotubes: effect of pH, Processes 7 (6) (2019) 1–9.
[14] L. Yang, L.E. Yu, M.B. Ray, Degradation of paracetamol in aqueous solutions by TiO2 photocatalysis, Water Res. 42 (13) (2008) 3480–3488.
[15] M. de los, M. Ballari, M.L. Satuf, O.M. Alfano, Photocatalytic reactor modeling: application to advanced oxidation processes for chemical pollution abatement, Springer International Publishing 377 (5) (2019).
[16] M. el M. Zekri, C. Colbeau-Justin, A mathematical model to describe the photocatalytic reality: what is the probability that a photon does its job? Chem. Eng. J. 225 (2013) 547–557.

[17] A. Manassero, M.L. Satuf, O.M. Alfano, Kinetic modeling of the photocatalytic degradation of clofibric acid in a slurry reactor, Environ. Sci. Pollut. Res. 22 (2) (2014) 926–937.
[18] M.L. Satuf, R.J. Brandi, A.E. Cassano, O.M. Alfano, Photocatalytic degradation of 4-chlorophenol: a kinetic study, Appl. Catal. B Environ. 82 (1–2) (2008) 37–49.
[19] M.J. Muñoz-Batista, M.M. Ballari, A. Kubacka, O.M. Alfano, M. Fernández-García, Braiding kinetics and spectroscopy in photo-catalysis: the spectro-kinetic approach, Chem. Soc. Rev. 48 (2) (2019) 637–682.
[20] A. Visan, J.R. Van Ommen, M.T. Kreutzer, R.G.H. Lammertink, Photocatalytic reactor design: guidelines for kinetic investigation, Ind. Eng. Chem. Res. 58 (14) (2019) 5349–5357.
[21] M.L. Satuf, R.J. Brandi, A.E. Cassano, O.M. Alfano, Quantum efficiencies of 4-chlorophenol photocatalytic degradation and mineralization in a well-mixed slurry reactor, Ind. Eng. Chem. Res. 46 (1) (2007) 43–51.
[22] C.C. Chen, C.S. Lu, Y.C. Chung, J.L. Jan, UV light induced photodegradation of malachite green on TiO2 nanoparticles, J. Hazard Mater. 141 (3) (2007) 520–528.
[23] L. Yang, L.E. Yu, M.B. Ray, Photocatalytic oxidation of paracetamol: dominant reactants, intermediates, and reaction mechanisms, Environ. Sci. Technol. 43 (2) (2009) 460–465.
[24] Q. Yang, P. Ling Ang, M.B. Ray, S.O. Pehkonen, Light distribution field in catalyst suspensions within an annular photoreactor, Chem. Eng. Sci. 60 (19) (2005) 5255–5268.
[25] J. Moreira, B. Serrano, A. Ortiz, H. De Lasa, Evaluation of photon absorption in an aqueous TiO2 slurry reactor using Monte Carlo simulations and macroscopic balance, Ind. Eng. Chem. Res. 49 (21) (2010) 10524–10534.
[26] T. Yokota, S. Cesur, H. Suzuki, H. Baba, Y. Takahata, Anisotropic scattering model for estimation of light absorption rates in photoreactor with heterogeneous medium, J. Chem. Eng. Japan 32 (3) (1999) 314–321.
[27] V. Pareek, S. Chon, M. Tadé, A. Adesoji, Light intensity distribution in heterogenous photocatalytic reactors, Asia-Pacific J. Chem. Eng. 3 (17) (2008) 171–201.
[28] A. Tolosana-Moranchel, J.A. Casas, J. Carbajo, M. Faraldos, A. Bahamonde, Influence of TiO2 optical parameters in a slurry photocatalytic reactor: kinetic modelling, Appl. Catal. B Environ. 200 (2017) 164–173.
[29] S. Yurdakal, et al., Optical properties of TiO2 suspensions: influence of pH and powder concentration on mean particle size, Ind. Eng. Chem. Res. 46 (23) (2007) 7620–7626.
[30] M.I. Cabrera, O.M. Alfano, A.E. Cassano, Absorption and scattering coefficients of titanium dioxide participate suspensions in water, J. Phys. Chem. 100 (51) (1996) 20043–20050.
[31] M.L. Satuf, R.J. Brandi, A.E. Cassano, O.M. Alfano, Experimental method to evaluate the optical properties of aqueous titanium dioxide suspensions, Ind. Eng. Chem. Res. 44 (2005) 6643–6649.